HYBRID ART FOR THREE-DIMENSIONAL LASER INTERFEROMETRIC CT (LICT) MEASUREMENT OF WAVE INTERACTION AROUND A RECTANGULAR ROD

TSUCHIKURA Sunao*, INAGE Tatsuro*, OTA Masanori,and MAENO Kazuo****
***Graduate Student, Graduate School of Enginnering, Chiba University**
****Graduate School of Engineering, Chiba University**
1-33 Yayoi, Inage, Chiba #263-8522 JAPAN
Fax: Jpn-(0)43-290-3220, Email: 09tm2145@graduate.chiba-u.jp

Keywords: *LICT measurement, shock wave, HART, unsteady flow*

Abstract

Laser Interferometric Computed Tomography (LICT) measurement is an useful method to observe high-speed unsteady flow field, and three-dimensional (3-D) density distribution is obtained. In our previous study, the flow fields which do not include objects was observed by LICT measurement, and the flow field was reconstructed by Filtered Back Projection (FBP) method, Algebraic Reconstruction Technique (ART), and so on. These CT images have less image artifacts, therefore various unsteady phenomena were clarified. However, the flow field including some objects is reconstructed with a lot of strong artifacts, therefore it is difficult to investigate various unsteady phenomena. These artifacts are thought to be due to lack of projection data because of some objects, therefore missing parts of projection data need to be interpolated by appropriate method. In this paper Hybrid Algebraic Reconstruction Technique (HART) is applied to LICT measurement to reduce these strong image artifacts. In HART the missing parts of projection data are interpolated from Computed Fluid Dynamics (CFD) model, and the flow field is reconstructed by ART from these interpolated projection data. The CT images reconstructed by HART are compared with the images reconstructed from imperfect data, and comparing the flow field reconstructed by HART with CFD model various unsteady phenomena are investigated.

1 Introduction

In recent years various high-speed unsteady flow fields including shock waves and vortices have been studied. Especially the simulations of unsteady flow by Computed Fluid Dynamic (CFD) are carried out in all over the world, and the three-dimensional (3-D) various unsteady phenomena are investigated. On the other hand, only two-dimensional (2-D) data are obtained by previous experimental visualization methods, such as shadowgraph, color-schlieren, and interferometric methods, therefore the 3-D data of unsteady flow field simulated by CFD could not to be compared with the experimental data strictly. Computed tomography (CT) methods are applied to the observation of 3-D flow fields. Subsonic and transonic free jets have been studied by interferometric holography [1], and also supersonic jets have been studied by C.Soller et al. [2]. These flow fields , however, are steady flow fields, and high-speed unsteady flow fields including shock waves and vortices have not been observed by experimental method. Laser Interferometric Computed Tomography (LICT) measurement is an useful visualization method to observe 3-D various unsteady phenomena. The LICT measurement is a combination of finite-fringe interferometory and multidirectional observation technique. In our previous study, the flow field including shock waves discharged from a square nozzle and the flow field including shock waves discharged from two parallel and cylindrical nozzle [3-6]

are observed by LICT measurement, and various 3-D unsteady phenomena are clarified. However, in LICT measurement N_2 pulse laser is used as a light source to obtain projection image data. Therefore if some objects were included in the flow field, the laser could not pass the objects, and imperfect projection image data is obtained. The CT images reconstructed from these imperfect data include strong artifacts, and it is difficult to investigate various unsteady phenomena. Actually the flow field including shock waves around circular cylinder [7] and the unsteady flow field around the rectangular rod [8] were observed by LICT measurement in our laboratory, however these reconstructed images of flow fields include a lot of artifacts. Most of these artifacts are caused by imperfect parts of projection data, therefore these imperfect parts caused by objects have to be interpolated by appropriate method. In this paper, to reduce these strong artifacts Hybrid Algebraic Reconstruction Technique (HART) is applied to LICT measurement as one of the reconstruction technique for reconstruction from imperfect projection data. HART is a combination of ART and CFD. The imperfect parts of projection data are interpolated from CFD model in HART. The HART is applied to reconstruction of the flow field around a rectangular rod, and the reconstructed CT images by HART are compared with the images reconstructed by ART and CFD model. These comparisons are used to evaluate HART and to investigate various unsteady phenomena.

2 Experimental Apparatus

2.1 Diaphragmless Shock Tube

A diaphragmless shock tube is used in LICT measurement to produce shock waves with good reproducibility. Figure 1 shows layout of the experimental apparatus. The cross section of the low-pressure tube is 40mm x 40mm square and the length of the low pressure tube is 3.1 meters. The driver gas is high-pressure helium and the test gas is low-pressure nitrogen. The incident Mach number M_i is calculated from pressure signals obtained by a pressure transducer as shown in Fig. 1. In this paper incident Mach number is fixed to 2.0 for the HART application.

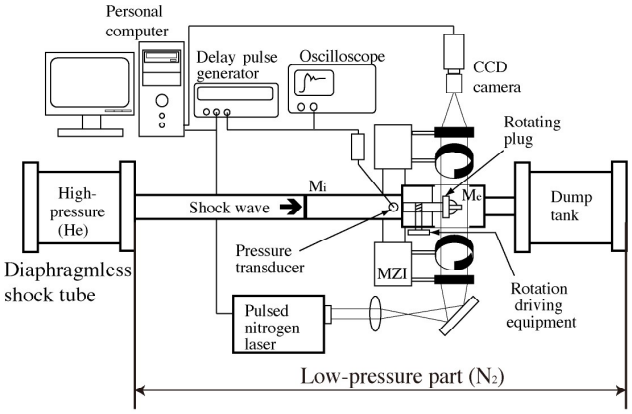

Fig.1 Layout of experimental apparatus

2.2 Rotation Model

A rotating plug is installed at end of low-pressure tube, and the rotation angle θ can be controlled from the rotation driving equipment that is out side of shock tube. The layout of the rotating plug is illustrated in Fig.2. In this paper the rotating plug that has a rectangular rod (4mm x 4mm x 10mm) and a circular nozzle (ϕ = 4mm) is used. Figure 3 shows coordinate system of the rotating plug. The x and y coordinates rotate with rotating plug around the z-axis, while light axis s is fixed with the shock tube, where rotation angle θ is defined as the angle between x-axis and s-axis. In this paper the rotation angle is set from 0 degree to 90 degree with 5 degree interval considering line-symmetry of the rotating plug.

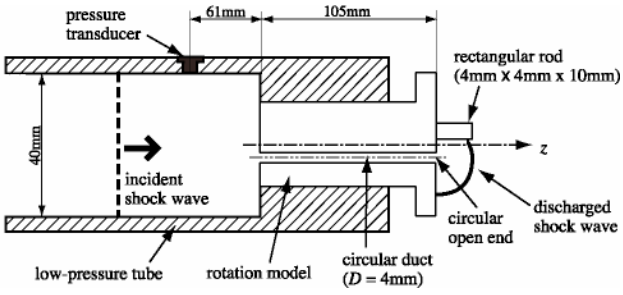

Fig.2 Layout of duct model

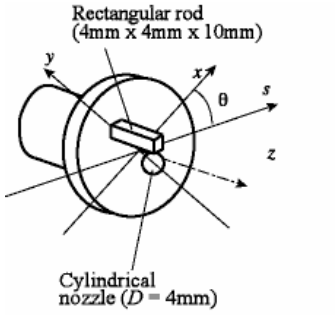

Fig.3 Coordinate system of rotating plug

2.3 Mach-Zehnder Observation System

Observation system consists of a Mach-Zehnder interferometer, a pulse nitrogen laser as a light source, a monochrome CCD camera, and a delay/pulse generator. The CCD plate is 640 x 512 pixels 2-D and diode array with 8-bit brightness level. The projection data of the flow field is obtained as a finite-fringe interferogram by the CCD camera, and each image is obtained at fixed rotation angle of rotating plug in each shot of experiment.

3 CT Measurement

3.1 Projection Data

As previously mentioned, each projection data is obtained in each shot of experiment in LICT measurement. Therefore, it is important to keep high accuracy of each experiment for the good quality CT image. To carry out experiment with enough accuracy, the normalized frontal position Z_s / D of the primary shock wave is defined as shown in Fig.4, where parameter D (=4mm) is diameter of a circular nozzle, and parameter Z_s is the position of primary shock wave measured as the axial position on the digitalized projection image. Corresponding to these parameters, accuracy of each experiment is enhanced. In this paper the accuracy of Z_s is within ±2 pixels on the CCD plate, and the accuracy of parameter Z_s / D (=2.77) is within 1.1%.

To obtain 3-D digitalized projection data of density distribution, each projection image have to be calculated by fringe-tracking method. Fringe tracking method is divided into three steps. First, fringe are tracked by tracking algorithm, secondly, the displacement ΔH of these fringes is obtained. Finally, integral quantity of density change is calculated according to the following expression,

$$\int (\rho - \rho_0) ds = \frac{\Delta H}{H_0} \times \frac{\lambda}{K} \qquad (1)$$

where ρ_0 is initial density distribution, H_0 is averaged initial distance of fringes, λ is wavelength of laser, and K is Gradstone-Dale constant.

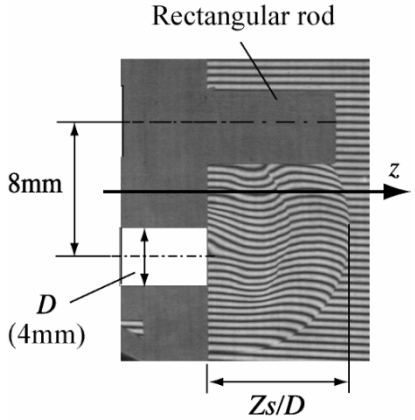

Fig.4 Position of Z_s / D in digitalized projection image

3.3 Hybrid Reconstruction Technique

In LICT measurement, experimental laser beam is used as a light source to obtain projection data. Therefore, if some objects were set in flow field, the light could not pass through the part of objects, and the lack parts of projection data are obtained. This situation is sometimes seen in fluid dynamics problems, where aerodynamics models are settled in the flow field. Theses imperfect parts of projection data are need to be interpolated by appropriate method, and the method should be based on physics or analytical consideration. In HART, these imperfect parts of the projection data are interpolated from CFD phantom. The CFD phantom is the 3-D density distribution of numerical simulation, and the flow field is reconstructed from these pseudo projection data. Figure 5 shows the projection data before interpolated and after interpolated. The gray part is interpolated part, and the boundary parts of experimental projection data and calculated projection data from CFD phantom are smoothed to reduce the noise caused by discontinuous parts. Pseudo

projection data consist of experimental and simulated projection data, therefore the reconstructed CT image represents hybrid data of experimental data and simulated data.

ART is used as the reconstruction technique for the reconstruction from these pseudo projection data. ART is one of the primitive reconstruction techniques. Filtered Back Projection (FBP) method is commonly used as the reconstruction technique, however noise levels of reconstructed CT images are low in case of ART than compared to FBP. Therefore, ART is useful reconstruction technique especially in case of the reconstruction using these pseudo projection data. If the area of object is included in reconstruction field, the boundary lines of objects and flow field are not presented sharply in HART. To solve this problem, the area of object is identified from imperfect part of projection data, and the area is excluded from the reconstructed field.

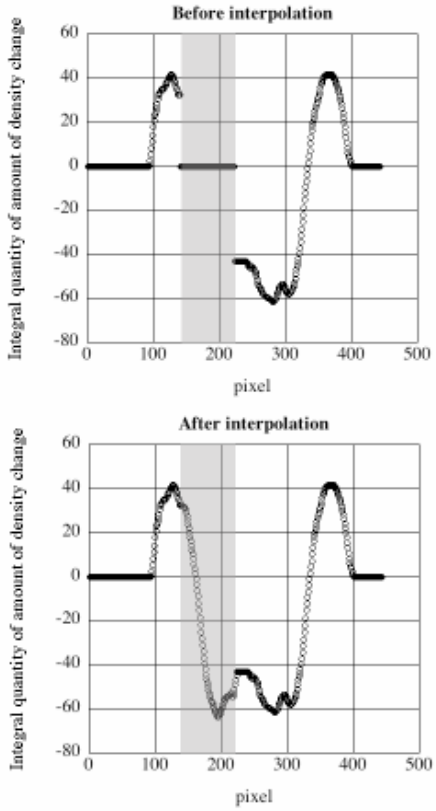

Fig.5 Experimental projection data and pseudo projection data (θ=30dgree, z/D=0.77)

4 Distribution Combined Schlieren Images (DCSI)

The experimental CT images are shown as the pseudo-color images, and these images represent density distribution. However it is hard to identify the position of discontinuous line or surface in these pseudo-color iamges. On the other hand, psedo-schliren technique is useful to identify these positions. DCSI is a fusion of pseudo-shliren image and pseudo-color image, therefore this novel expression method shows not only density distribution but also the positions of discontinuous line and surface clearly. This method was suggested by Ota et al.[9] , and it is much easier to understand the structure of shock waves and flow field.

5 Numerical Simulation (CFD phantom)

Imperfect part of the projection data is interpolated from CFD phantom in HART. CFD phantom is calculated with numerical simulation for inviscid and compressible unsteady flow. The basic equations are Euler equation for inviscid and compressible flows assumed as perfect gas. The equation system is solved with Harten-Yee type second-order up wind TVD scheme. The third-order Runge-Kutta method was applied to time integration. Initial exit Mach number of shock wave is fixed to 2.4. Orthogonal grid is used as computational grid and the size of grid is 105 x 105 x 105.

6 Results and Discussion

In this section, the CT images reconstructed by HART and by ART are shown, and CFD phantom is also shown as not only the model but also the results of computational simulation. Experimental conditions are set as follows. The incident Mach number M_i is 2.0, and the normalized frontal position of primary shock wave Z_s / D is 2.77, where diameter of a circular nozzle D is 4mm.

The CFD phantom is shown in Fig.6. The position A-H shown in the fig.6 are the position of x-y cross section (A-F) and y-z cross section (G-H), and these cross sections are used to compare the results reconstructed by HART and ART in this section. The normalized position of cross section z / D are as follows; A: 2.00, B:

1.53, C: 1.38, D: 1.23, E: 1.08, F: 0.77, and *y-z* cross section G is central cross section of rectangular rod while H is the cross section on the corner of rectangular rod.

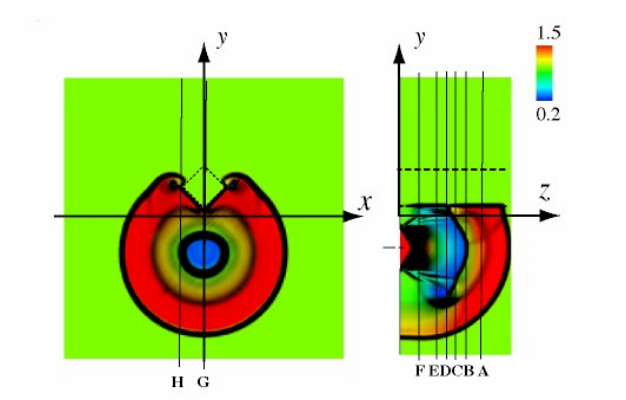

Fig.6 CFD phantom

The *y-z* cross section of CT images reconstructed by ART and by HART and CFD results are shown in fig.7 and fig.8, where the position of cross section is on G in fig.7, and the *y-z* cross section on H is shown in fig.8. In fig.7 both images reconstructed by ART and by HART show several unsteady phenomena, for example, the primary shock wave (PSW), the secondary shock wave (SSW), and vortex are clearly observed. The secondary shock wave is categorized into four types SSW1, SSW2, SSW3, and SSW4, where these types of secondary shock wave were categorized by Maeno et al.[10]. Both CT images reconstructed by HART and ART show these unsteady phenomena in fig.7 and fig.8. In fig.7 the difference is small between the CT images reconstructed by ART and HART, and the various unsteady phenomena are reconstructed in both CT images. In fig.8, however, the CT image reconstructed by HART shows several unsteady phenomena near the rectangular rod more clearly. For example PSW above the rectangular rod is identified in the image reconstructed by HART. In addition, the vortex and CS under the rectangular rod are also shown in same image. The reflected shock wave (RSW), however, is shown in only the images of CFD phantom, and the RSW is not observed in both CT images.

The *x-y* cross sections of the CFD phantom and CT images reconstructed by ART and HART are shown in fig.9 (on A-C) and fig.10 (on D–F). Various unsteady phenomena are shown in both CT images reconstructed by ART and HART. The PSW, SSW1, SSW4, and CS are observed in several CT images and CFD phantom. The CT images reconstructed by ART, however, show strong artifacts, and the shapes of SSW1, SSW4, PSW, and CS are not identified especially near the rectangular rod. On the other hand, these phenomena are identified in HART, and the structure of the unsteady flow field is shown more clearly. For example, the PSW around a rectangular rod is shown in several CT images reconstructed by HART, and SSW4 and vortex under the rectangular rod are shown in the *x-y* cross section on F. These phenomena are observed in the CT images reconstructed by ART, however these shapes are broken, therefore it is difficult to identify the various unsteady phenomena especially near the rectangular rod. Various phenomena are observed in the CT images reconstructed by HART, however several unsteady phenomena is shown in the images of CFD phantom. For example, RSW is not shown in both CT images reconstructed by ART and HART, and also the CS is not observed clearly in the both CT images. Especially CS is not shown clearly in the several *x-y* cross sections, for example, the cross sections on C and D show CS more clearly in the case of ART than compared to HART at the distant area from rectangular rod. This is attributed to the fact that the CT images reconstructed by HART include the hybrid data of experimental data and simulated data. The simulated data not correspond to the experimental data, therefore the hybrid data have possibility that one data blur the another data. Therefore the simulated projection data should be controlled by appropriate functions, and the experimental data should be reconstructed more dominantly than simulated projection data.

7 Conclusion

HRT have successfully applied to the LICT measurement of the unsteady flow field including shock waves around a rectangular rod. The imperfect parts of the projection data have

interpolated from CFD phantom in HART, and the image artifacts have reduced. Therefore, various phenomena have been observed especially near the rectangular rod. For example, PSW around the object, CS and vortex under the rectangular rod were observed. However, RSW was not observed in CT images, and only the images of CFD phantom showed RSW. In addition various unsteady phenomena were shown more clearly in case of ART than HART at the distance of the rectangular rod. This is attributed to the fact that the CT images reconstructed by HART include the hybrid data of experimental data and simulated data. Therefore the simulated projection data should be controlled by appropriate functions, and the experimental data should be reconstructed more dominantly than simulated projection data.

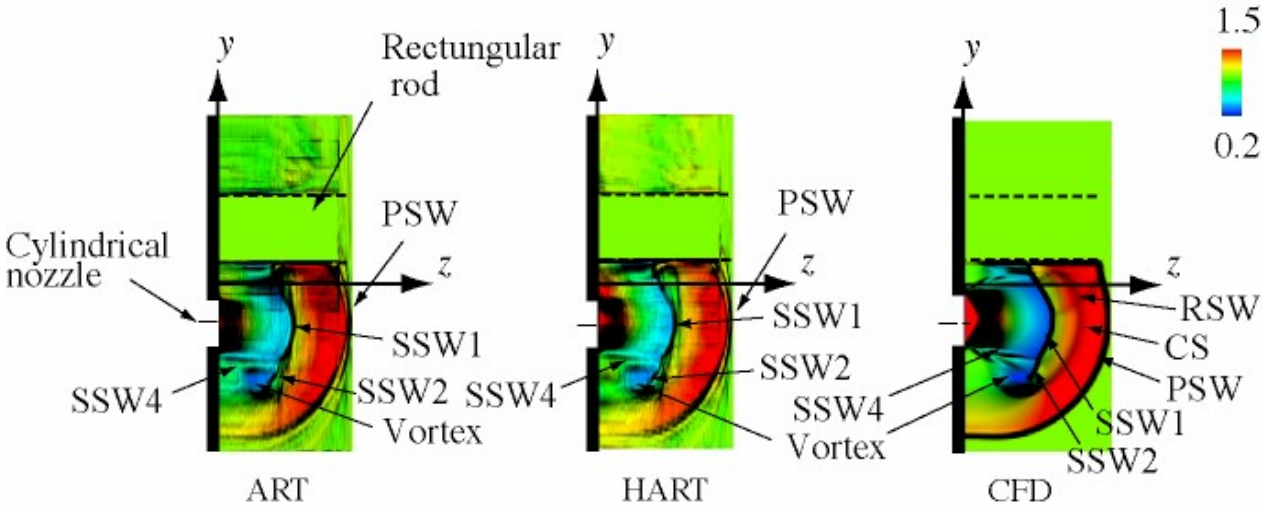

Fig.7 CT images and CFD result (*y*-*z* cross section on G)

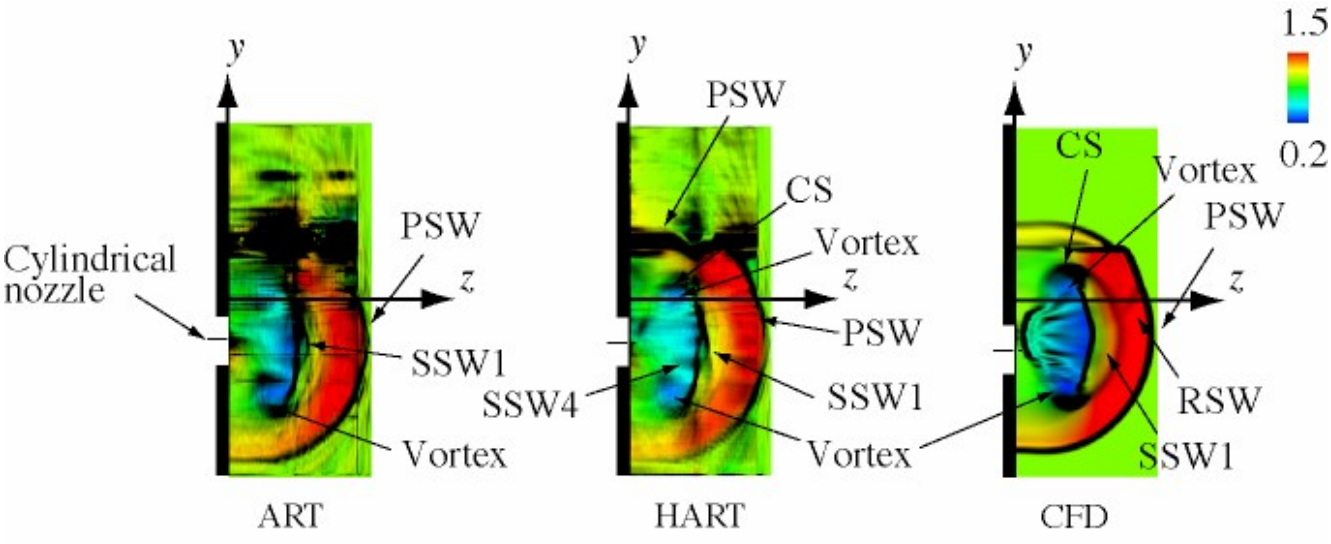

Fig.8 CT images and CFD result (*y*-*z* cross section on H)

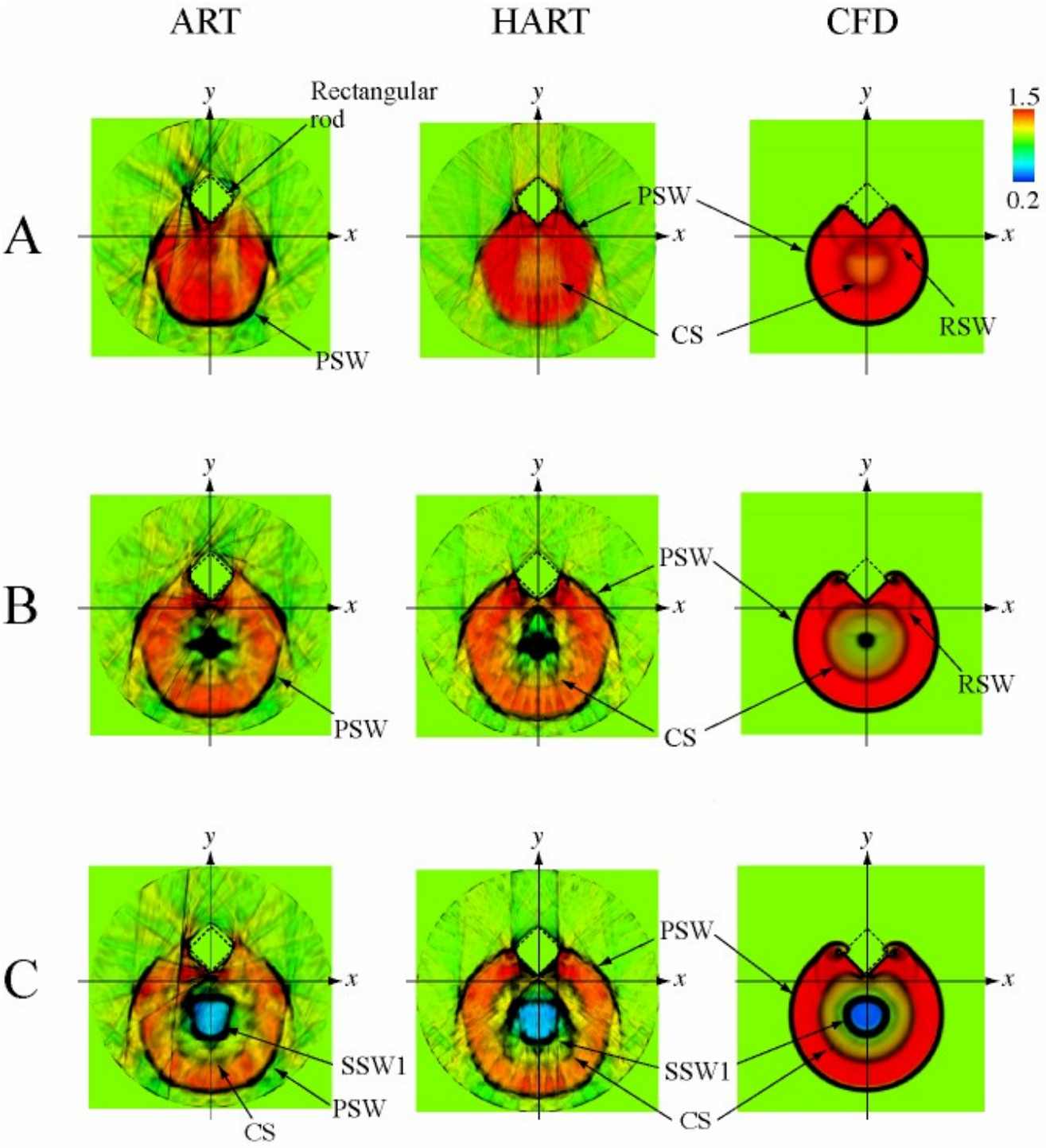

Fig.9 CT images and CFD result (*x*-*y* cross section on A-C)

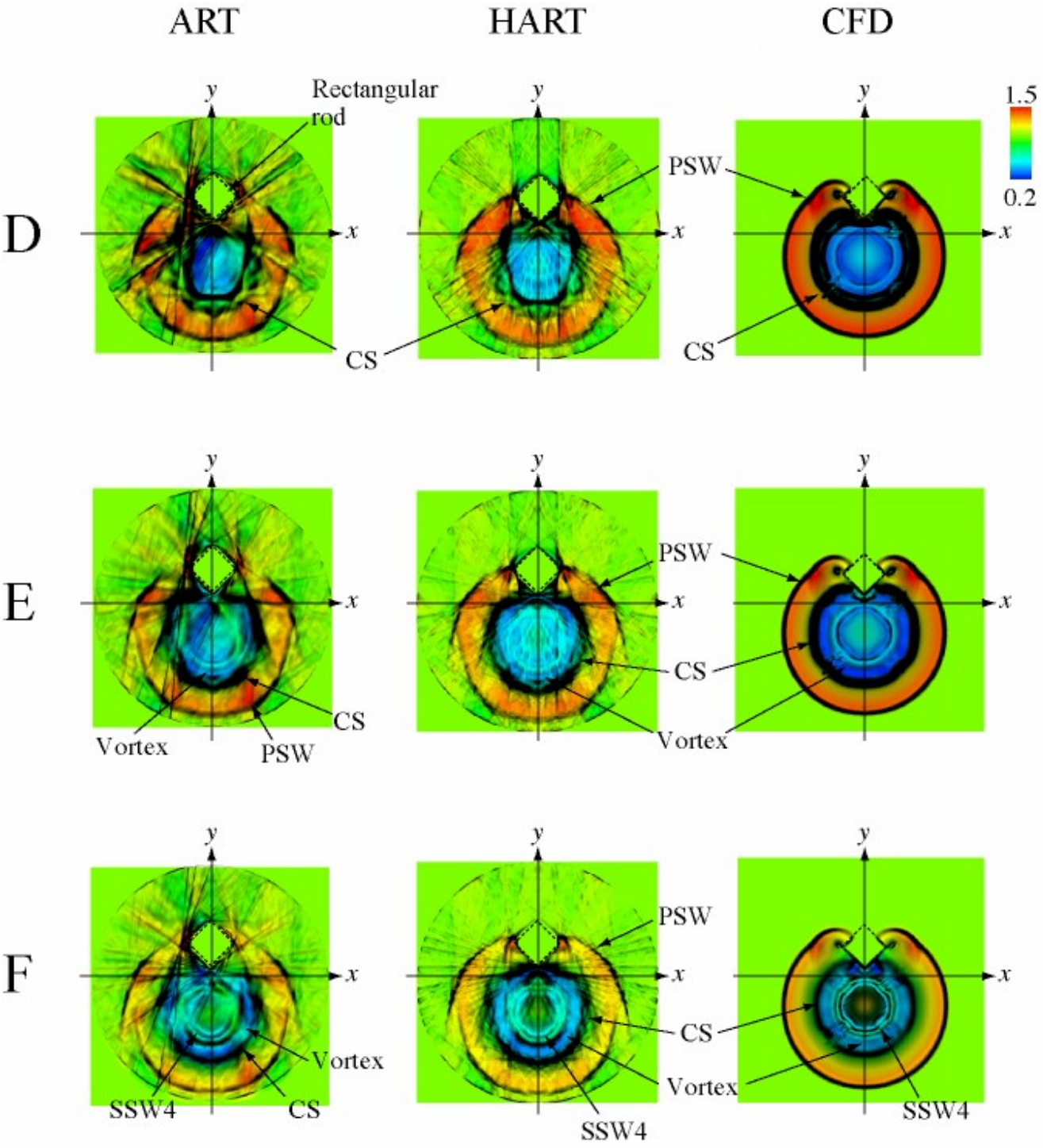

Fig.9 CT images and CFD result (*x*-*y* cross section on D-F)

References

[1] L. T. Clark, D. C. Koepp, and J. J. Thykkuttathil, Three-dimensional density field measurement of a transonic flow from a square nozzle using holographic interferometry, *J. Fluids Eng. 99*, pp 737-744, 1977.

[2] C. Soller, R. Wenskus, P. Middendorf, G. E. A. Meier, and F. Obermeier, Interferometric tomography for flow visualization of density fields in supersonic jets and convective flow, *Appl. Opt.* vol. 33, No. 14, 1994.

[3] H. Honma, M. Ishihara, T. Yoshimura, K. Maeno, Interferometric CT measurement of three-dimensional flow phenomena on shock waves and vortices discharged from open ends, *Shock Waves*, 13, pp.179-190. 2003.

[4] T. Yoshimura, M. Ishihara. T. Asahina, K. Maeno, H. Honma, Interferometric CT measurements of 3-D shock wave phenomena. A square open end, *Proc. Of Sym. Of Shock Waves in Japan*, pp.141-144. 2000.

[5] H. Honma, M. Ishihara, T. Yoshimura, T. Asahina, K. Maeno, Interferometric CT measurements of 3-D shock wave phenomena. A pair of circular open end, *Proc. of Sym. Of Shock Waves in Japan*, pp.145-148. 2000.

[6] M. Ota, T. Koga, K. Maeno, Laser interferometric CT measurement of the unsteady supersonic shock-vortex flow field discharging from two parallel and cylindrical nozzle, *Measurement Science and Technology, 17*, pp. 2066-2071, 2006.

[7] M. Ota, T. Inage, K. Maeno, An extension of laser-interferometric CT measurement to unsteady shock waves and 3D flow around a columnar object, Flow *Meas. Instrum. 18*, pp. 295-300, 2007.

[8] T. Inage, M. Ota, K. Maeno, Laser-interferometric CT measurement of discharging shock waves and unsteady flow field around a rectangular rod, *International Sym. on Flow Visualization 13th*, Nice, France, pp. 1-8, 2008.

[9] M. Ota, T. Koga, K. Maeno, Interferometric CT measurement and novel expression method of discharged flow field with unsteady shock waves, *Japanese Journal of Applied Physics*, Vol. 44, pp. 1293-1294, 2005.

[10] K. Maeno, T. Kaneta, T. Yoshimura, T. Morioka, and H. Honma, Pseudo-schlieren CT measurement of three-dimensional flow phenomena on shock waves and vortices discharged from open ends, *Shock Waves* 14, pp. 239-249, 2005.

Contact Author Email Address

Tsuchikura Sunao
E-mail: 09tm2145@graduate.chiba-u.jp

Copyright Statement